Available online at www.sciencedirect.com
ScienceDirect
Journal of Sound and Vibration 310 (2008) 493–511
JOURNAL OF SOUND AND VIBRATION
www.elsevier.com/locate/jsvi

An alternative approach for the analysis of nonlinear vibrations of pipes conveying fluid

Michael Stangl*, Johannes Gerstmayr, Hans Irschik

Institute of Technical Mechanics, Johannes Kepler University Linz, Altenbergerstrasse 69, A-4040 Linz, Austria

Accepted 18 June 2007
The peer review of this article was organised by the Guest Editor
Available online 4 September 2007

Abstract

Based on a novel extended version of the Lagrange equations for systems containing non-material volumes, the nonlinear equations of motion for cantilever pipe systems conveying fluid are deduced. An alternative to existing methods utilizing Newtonian balance equations or Hamilton's principle is thus provided. The application of the extended Lagrange equations in combination with a Ritz method directly results in a set of nonlinear ordinary differential equations of motion, as opposed to the methods of derivation previously published, which result in partial differential equations. The pipe is modeled as a Euler elastica, where large deflections are considered without order-of-magnitude assumptions. For the equations of motion, a dimensional reduction with arbitrary order of approximation is introduced afterwards and compared with existing lower-order formulations from the literature. The effects of nonlinearities in the equations of motion are studied numerically. The numerical solutions of the extended Lagrange equations of the cantilever pipe system are compared with a second approach based on discrete masses and modeled in the framework of the multibody software HOTINT/MBS. Instability phenomena for an increasing number of discrete masses are presented and convergence towards the solution for pipes conveying fluid is shown.

1. Introduction

The dynamics of fluid conveying pipes has been the subject of a large number of scientific investigations over the last 60 years. Starting with the linear equations of motion for pipes supported at both ends by Feodos'ev and Housner in the 1950s, several refined models have been presented leading to a full nonlinear model of a cantilever conveying fluid by Semler et al. [2]. For a comprehensive overview, see Païdoussis [1,3] and for own contributions [4–6]. The stability analysis performed by varying parameters of the resulting equations of motion has been subject of intensive research, and a recent survey on bifurcations in nonlinear models for pipes supported at both ends can be found in Ref. [7], and for cantilevered pipes in Ref. [8]. In most cases, the derivation of the equations of motion is either based on a Newtonian approach, see e.g. [9–11] or an energy-based approach applying an extended version of Hamilton's principle, first introduced by Benjamin

*Corresponding author. Tel.: +43 70 24689765; fax: +43 70 24689763.
E-mail address: michael.stangl@jku.at (M. Stangl).

0022-460X/$ - see front matter © 2007 Elsevier Ltd. All rights reserved.
doi:10.1016/j.jsv.2007.06.020

[12], see e.g. [1,2]. Both approaches result in a partial differential equation (PDE) for the equation of motion of the pipe system. The derivations often include order-of-magnitude considerations for the longitudinal and transverse deflection of the pipe resulting in an equation of motion valid for sufficiently small deflections of the pipe. The common way for solving the equation of motion is a Galerkin approximation requiring an integration of the nonlinear PDE over the pipe domain.

The work presented here provides an alternative approach for deriving the equations of motion for pipe systems. The example of a cantilevered pipe conveying fluid is considered, and a generalized form of the Lagrange equations for systems containing non-material volumes, as presented by Irschik and Holl in Ref. [13], in combination with a Ritz method, is applied. This brings up the possibility of an easy implementation in existing multibody codes. In order to derive equations of motion eligible for modeling large deformations of the pipe, no order-of-magnitude considerations will be applied first. A novel feature of the presented modeling is the possibility of selecting arbitrary order of approximation of the final equations of motion afterwards, contrary to existing formulations, in which the order of the final equations is a priori defined and corresponding order-of-magnitude considerations are applied throughout the derivation. In the present paper, the resulting equations are solved using the implicit Runge–Kutta solver HOTINT [14], applying high-order Gauss–Legendre integration. The results are compared with existing works and the influence of high-order terms in the equations of motion on the dynamics and stability of the system is discussed. In a second step, the solution of the equations of motion derived from the extended Lagrange equations is compared with the solution obtained from the multibody code HOTINT/MBS.[1] This multibody code is used to compute the solution for a cantilevered pipe modeled by deformable bodies with additional sliding masses. The effects of increasing numbers of masses sliding through the pipe are studied.

2. Modeling of the cantilever pipe system

The pipe shown in Fig. 1 is modeled as a Euler elastica, i.e. nonlinear Bernoulli–Euler-type beam theory is applied assuming an inextensible centerline [15], with uniform cross-sectional area A_P and length L, constant mass per unit length m and constant bending stiffness EI. Its diameter is assumed to be small relative to the length of the pipe, and, in accordance with the Bernoulli–Euler hypothesis, transverse shear deformation and rotatory inertia are neglected. Planar motions of the pipe undergoing large deflections are investigated. In accordance with numerous existing works, see e.g. [1,16,17], the internal flow of fluid is taken into account as a plug flow, i.e. with a uniform velocity profile, moving at velocity U relative to the pipe, where secondary flow effects are neglected and the fluid is considered as incompressible.

In the following derivation, the strain energy due to elastic deformation of a Euler elastica pipe is first deduced in terms of the displacement field. Based on an exact planar nonlinear beam theory, the strain energy for the Euler elastica pipe follows by consequent application of the inextensibility condition. The position vector $\mathbf{r}_0$ of a point on the deformed pipe axis in the Lagrangian description reads

$$\mathbf{r}_0 = \begin{pmatrix} X+u \\ w \end{pmatrix}, \tag{1}$$

where X represents the spatial coordinate in the undeformed reference configuration, $u = u(X,t)$ and $w = w(X,t)$ are the axial and transverse displacements of the pipe axis, respectively. Introducing the abbreviations $(\,)' = \partial(\,)/\partial X$ and $(\,^\bullet) = \partial(\,)/\partial t$, the axial strain $\varepsilon_{xx}(Z=0)$ of the pipe axis is computed by

$$\varepsilon_{xx}(Z=0) = \frac{1}{2}\frac{\partial \mathbf{r}_0}{\partial X}\cdot\frac{\partial \mathbf{r}_0}{\partial X} - \frac{1}{2} = \frac{1}{2}\left(2u' + u'^2 + w'^2\right), \tag{2}$$

where Z denotes the distance from the deformed and undeformed beam axis in direction of the normal unit vector $\boldsymbol{\nu}$ of the deformed axis:

$$\boldsymbol{\nu} = \frac{1}{\sqrt{1+2\varepsilon_{xx}(Z=0)}}\begin{pmatrix} -w' \\ 1+u' \end{pmatrix}. \tag{3}$$

[1]Details at: ⟨http://tmech.mechatronik.unilinz.ac.at/staff/gerstmayr/hotint.html⟩.

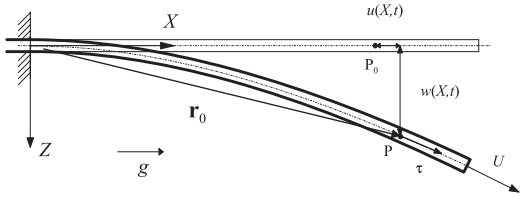

Fig. 1. Cantilevered elastica pipe with internal flow U.

Applying the kinematic hypothesis of the Euler elastica theory, assuming that plane cross-sections of the pipe that are perpendicular to the undeformed pipe axis remain plane and perpendicular to the deformed pipe axis, the position vector of a point on the pipe in the deformed state thus reads

$$\mathbf{r} = \mathbf{r}_0 + Z\mathbf{v}. \tag{4}$$

The approach shown in Eq. (4) has also been proposed by Simo and Vu Quoc in Ref. [18], where flexible beams under large overall motions were investigated. The deformation gradient tensor $\mathbf{F}$, see e.g. Malvern [19], is defined as the tensor whose rectangular Cartesian components are the partial derivatives of the position vector $\mathbf{r}$ with respect to the Lagrangian coordinates X and Z in the undeformed reference configuration

$$\mathbf{F} = \left(\frac{\partial \mathbf{r}}{\partial X} \quad \frac{\partial \mathbf{r}}{\partial Z}\right) = \mathrm{Grad}(\mathbf{r}) = \begin{pmatrix} 1 + u' - \dfrac{Zw''}{\sqrt{1+2\varepsilon_{xx}(Z=0)}} & -\dfrac{w'}{\sqrt{1+2\varepsilon_{xx}(Z=0)}} \\ w' + \dfrac{Zu''}{\sqrt{1+2\varepsilon_{xx}(Z=0)}} & \dfrac{1+u'}{\sqrt{1+2\varepsilon_{xx}(Z=0)}} \end{pmatrix}. \tag{5}$$

Green's strain tensor follows

$$\mathbf{E} = \frac{1}{2}(\mathbf{F}^{\mathrm{T}}\mathbf{F} - \mathbf{I}) = \begin{pmatrix} \varepsilon_{xx} & 0 \\ 0 & 0 \end{pmatrix} \tag{6}$$

with $\mathbf{I}$ denoting the identity matrix. The axial strain of a pipe element in a distance Z from the pipe axis is

$$\varepsilon_{xx} = \frac{1}{2}(1 + 2\varepsilon_{xx}(Z=0))\left[1 - 2Z\frac{(1+u')w'' - w'u''}{\sqrt{(1+2\varepsilon_{xx}(Z=0))^3}}\right] - \frac{1}{2}. \tag{7}$$

For cantilever pipe systems, as discussed by Païdoussis [1], Folley and Bajaj [9] or Troger and Steindl [10], the centerline of the pipe can be considered as inextensible. A beam with inextensible centerline is also referred as Euler elastica [15]. An inextensible centerline corresponds to a vanishing axial strain of the pipe axis

$$\varepsilon_{xx}(Z=0) = 0. \tag{8}$$

Substituting Eq. (8) into Eq. (2) results in the following relationship between the spatial derivatives of the axial displacement u and the transverse displacement w:

$$(1+u')^2 + (w')^2 = 1. \tag{9}$$

The latter relation is called "inextensibility condition", see e.g. [2,15,20]. Inserting Eq. (8) into Eq. (7) and using Eq. (9) to eliminate the axial displacement u, the axial strain for a fiber in distance Z from the pipe axis of a Euler elastica pipe reads

$$\varepsilon_{xx} = -Z[(1+u')w'' - w'u''] = -Z\left[w''\sqrt{1-w'^2} + w'\frac{w'w''}{\sqrt{1-w'^2}}\right] = -Z\frac{w''}{\sqrt{1-w'^2}}. \tag{10}$$

In the next step, the terms necessary for setting up the Lagrange equations of motion for the cantilever elastica pipe with an internal flow of fluid will be deduced. In existing works, e.g. [1,16], the derivation of the strain energy is often based on an exact formulation of the curvature, but when setting up the energy expressions, the curvature terms are transformed into Taylor series and truncated after the first element.

The latter order-of-magnitude approximations for the strain energy will be omitted in the present work, and a general nonlinear formulation will be presented.

The local velocity vector of the fluid is set up by means of the tangent unit vector $\boldsymbol{\tau}$ of the deformed pipe and is multiplied by the scalar fluid velocity U, in accordance with the plug-flow assumption. The tangent unit vector $\boldsymbol{\tau}$ along the deformed pipe axis, using the spatial derivative of $\mathbf{r}_0$ in combination with Eq. (9), follows

$$\boldsymbol{\tau} = \left\| \frac{\partial \mathbf{r}_0}{\partial X} \right\|^{-1} \frac{\partial \mathbf{r}_0}{\partial X} = \begin{pmatrix} 1+u' \\ w' \end{pmatrix}, \tag{11}$$

where $||\cdot||$ denotes the ℓ^2-norm of a vector with components x_i defined by

$$\|\cdot\| = \sqrt{\sum_i x_i^2}. \tag{12}$$

As common in elastica theory, rotatory inertia terms will not be included in the kinetic energy, and therefore the velocity vector $\mathbf{v}_p$ of the pipe can be set equal to the velocity of the centerline

$$\mathbf{v}_P = \frac{\partial \mathbf{r}_0}{\partial t} = \begin{pmatrix} \dot{u} \\ \dot{w} \end{pmatrix}. \tag{13}$$

The velocity vector $\mathbf{v}_F$ of the fluid consists of two parts. One is due to the motion of the pipe $\mathbf{v}_p$, and the other is due to the relative motion of the fluid. Using the tangent unit vector from Eq. (11), one obtains

$$\mathbf{v}_F = \mathbf{v}_P + U\boldsymbol{\tau} = \begin{pmatrix} \dot{u} + U(1+u') \\ \dot{w} + Uw' \end{pmatrix}. \tag{14}$$

The kinetic energy of the pipe T_p can be written, using $\mathbf{v}_p$ from Eq. (13), as

$$T_P = \frac{1}{2} m \int_0^L \mathbf{v}_p^{\mathrm{T}} \mathbf{v}_P \, \mathrm{d}X = \frac{1}{2} m \int_0^L (\dot{u}^2 + \dot{w}^2) \, \mathrm{d}X, \tag{15}$$

where m is the mass of the solid pipe per unit length. The kinetic energy of the fluid T_F follows with Eq. (14) to

$$T_F = \frac{1}{2} M \int_0^L \mathbf{v}_F^{\mathrm{T}} \mathbf{v}_F \, \mathrm{d}X = \frac{1}{2} M \int_0^L \left((\dot{u} + U(1+u'))^2 + (\dot{w} + Uw')^2 \right) \mathrm{d}X \tag{16}$$

with M denoting the mass per unit length of the fluid. The potential energy due to gravitation V_g can be written as

$$V_g = -\begin{pmatrix} g & 0 \end{pmatrix}^{\mathrm{T}} (m+M) \int_0^L \mathbf{r}_0 \, \mathrm{d}X = -g(m+M) \int_0^L (X+u) \, \mathrm{d}X, \tag{17}$$

where g denotes the acceleration due to gravity which is acting in X direction, see Fig. 1. The potential energy due to elastic deformation V_e of the elastica pipe can be deduced using the axial strain of Eq. (10) and follows

$$V_e = \frac{1}{2} E \int_0^L \int_{A_P} \varepsilon_{xx}^2 \, \mathrm{d}A_P \, \mathrm{d}X = \frac{1}{2} \mathrm{EI} \int_0^L \frac{w''^2}{1-w'^2} \, \mathrm{d}X \tag{18}$$

with A_P denoting the cross-sectional area of the pipe. The total potential energy V of the system is computed by

$$V = V_g + V_e. \tag{19}$$

3. Lagrange equations of motion for systems containing non-material volumes

Further derivations will be based on a formulation of the Lagrange equations of motion written in a form capable of treating systems containing non-material volumes, first proposed by Irschik and Holl [13]. A non-material volume has a surface that moves relatively to the material particles instantaneously located at this surface, and is also denoted as moving control volume in the terminology of fluid mechanics, or as an open

system. In the present work, this control volume surrounds a fluid moving in a pipe system. In addition to the classical terms of the Lagrange equations, the new formulation includes additional terms in order to treat the fact that moving mass enters and exits the boundaries of the system. Thus, it represents an extension of the classical theory. Since most of the existing works [1,2,7] are based on an extended Hamilton principle for open systems, introduced by Benjamin [12], leading to PDEs of motion, the current work shows an alternative approach for investigating the dynamics of pipe systems. Hamilton's principle for open systems was deduced by application of Reynolds' transport theorem to the classical form of Hamilton's principle for a moving control volume where mass was assumed to be transported through its boundaries, as stated by Païdoussis [1]. The present extension of the classical Lagrange equations, in order to treat systems containing non-material volumes, uses a generalization of Reynolds' theorem concerning partial derivatives of the transported quantities with respect to a set of generalized coordinates and generalized velocities. The proposed approach offers a convenient tool for computational mechanics since the Lagrange equations are a common formulation in the latter field for obtaining the equations of motion in form of ordinary differential equations [21] that can be solved by means of standard time-integration codes [22,23].

The Lagrange equations for systems containing non-material volumes, as introduced in Ref. [13], can be written in the form

$$\frac{\mathrm{d}}{\mathrm{d}t}\frac{\partial T_w}{\partial \dot{q}_i}-\frac{\partial T_w}{\partial q_i}+\int_S \mathrm{d}\mathbf{a}\cdot(\mathbf{v}_F-\mathbf{v}_P)\frac{\partial T'}{\partial \dot{q}_i}-\int_S \mathrm{d}\mathbf{a}\cdot\left(\frac{\partial \mathbf{v}_F}{\partial \dot{q}_i}-\frac{\partial \mathbf{v}_P}{\partial \dot{q}_i}\right)T'-Q_i=0. \tag{20}$$

Here, T_w denotes the total kinetic energy contained in the control volume, however, taking into account that the surface of the latter moves at velocity $\mathbf{v}_P$ that is different from the particles located on it; for details see Irschik and Holl [13]. Owing to the present assumption of a plug flow in the pipe, we simply can set

$$\frac{\mathrm{d}}{\mathrm{d}t}\frac{\partial T_w}{\partial \dot{q}_i}=\frac{\mathrm{d}}{\mathrm{d}t}\frac{\partial}{\partial \dot{q}_i}(T_P+T_F),\quad \frac{\partial}{\partial q_i}T_w=\frac{\partial}{\partial q_i}(T_P+T_F). \tag{21}$$

Two surface integrals are included in the equations of motion in order to take into account mass transport. The surface integrals need to be evaluated at those parts of the boundary S, where mass enters or exits the system. In the investigated pipe system the inlet and the outlet surfaces of the pipe contribute to these integrals only. The vector $\mathrm{d}\mathbf{a}=\boldsymbol{\tau}\,\mathrm{d}A$ in Eq. (20) denotes an oriented surface element on S, where the cross-sectional area of the fluid in the pipe is denoted as A, as shown for the pipe outlet in Fig. 2. For the kinetic energy of the pipe and the fluid follows

$$\frac{\mathrm{d}}{\mathrm{d}t}\left(\frac{\partial T_P}{\partial \dot{q}_i}\right)=m\int_0^L\left(\ddot{u}\frac{\partial \dot{u}}{\partial \dot{q}_i}+\ddot{w}\frac{\partial \dot{w}}{\partial \dot{q}_i}\right)\mathrm{d}X, \tag{22}$$

$$\frac{\mathrm{d}}{\mathrm{d}t}\left(\frac{\partial T_F}{\partial \dot{q}_i}\right)=M\int_0^L\left((\ddot{u}+U\dot{u}')\frac{\partial \dot{u}}{\partial \dot{q}_i}+(\ddot{w}+U\dot{w}')\frac{\partial \dot{w}}{\partial \dot{q}_i}\right)\mathrm{d}X, \tag{23}$$

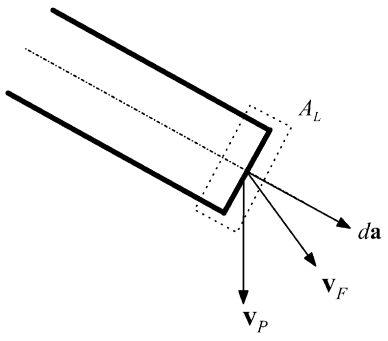

Fig. 2. Pipe outlet.

$$\frac{\partial T_P}{\partial q_i} = 0, \tag{24}$$

$$\frac{\partial T_F}{\partial q_i} = MU \int_0^L \left((\dot{u} + U(1+u')) \frac{\partial u'}{\partial q_i} + (\dot{w} + Uw') \frac{\partial w'}{\partial q_i} \right) \mathrm{d}X, \tag{25}$$

where q_i and $\dot{q}_i$ denote a set of generalized coordinates and velocities, respectively.

The generalized forces Q_i of the pipe system follow with Eq. (19) to

$$Q_i = -\frac{\partial V}{\partial q_i}. \tag{26}$$

The density of kinetic energy transported by a fluid particle, i.e. the kinetic energy per unit volume, denoted by T', is given as

$$T' = \tfrac{1}{2}\rho_F \mathbf{v}_F^{\mathrm{T}} \mathbf{v}_F = \tfrac{1}{2}\rho_F (\dot{u} + U(1+u'))^2 + \tfrac{1}{2}\rho_F (\dot{w} + Uw')^2 \tag{27}$$

with ρ_F representing the mass density of the fluid. The local partial derivative of T' with respect to the generalized velocities $\dot{q}_i$ follows

$$\frac{\partial T'}{\partial \dot{q}_i} = \rho_F (\dot{u} + U(1+u')) \frac{\partial \dot{u}}{\partial \dot{q}_i} + \rho_F (\dot{w} + Uw') \frac{\partial \dot{w}}{\partial \dot{q}_i}. \tag{28}$$

Evaluating Eq. (28) for $X = 0$ yields

$$\left. \frac{\partial T'}{\partial \dot{q}_i} \right|_{X=0} = 0, \tag{29}$$

since for the cantilever pipe system

$$\left. \frac{\partial \dot{u}}{\partial \dot{q}_i} \right|_{X=0} = 0 \quad \text{and} \quad \left. \frac{\partial \dot{w}}{\partial \dot{q}_i} \right|_{X=0} = 0. \tag{30}$$

Hence, there is no contribution to the equations of motion, since the corresponding surface integral in Eq. (20) is found to be

$$\int_{A_0} \mathrm{d}\mathbf{a} \cdot (\mathbf{v}_F - \mathbf{v}_P) \left. \frac{\partial T'}{\partial \dot{q}_i} \right|_{X=0} = 0 \tag{31}$$

with A_0 denoting the cross-surface area of the fluid for $X = 0$. Moreover, the second integral in Eq. (20) vanishes. It includes the partial derivatives of the velocity vectors of the pipe and of the fluid, $\mathbf{v}_F$ and $\mathbf{v}_P$, with respect to the generalized velocities $\dot{q}_i$. Since the tangent unit vector $\boldsymbol{\tau}$ in $\mathbf{v}_F$ from Eq. (14) has no dependency on $\dot{q}_i$, it follows that

$$\left(\frac{\partial \mathbf{v}_F}{\partial \dot{q}_i} - \frac{\partial \mathbf{v}_P}{\partial \dot{q}_i} \right) = \frac{\partial}{\partial \dot{q}_i} (U\boldsymbol{\tau}) = 0, \tag{32}$$

everywhere within the pipe. Hence, for the investigated pipe system, there is no contribution to the equations of motion from the second surface integral in Eq. (20) yielding

$$\int_{A_0} \mathrm{d}\mathbf{a} \cdot \left(\frac{\partial \mathbf{v}_F}{\partial \dot{q}_i} - \frac{\partial \mathbf{v}_P}{\partial \dot{q}_i} \right) T' = \int_{A_L} \mathrm{d}\mathbf{a} \cdot \left(\frac{\partial \mathbf{v}_F}{\partial \dot{q}_i} - \frac{\partial \mathbf{v}_P}{\partial \dot{q}_i} \right) T' = 0, \tag{33}$$

where A_L denotes the cross-surface area of the fluid for $X = L$. A non-vanishing contribution, however, is obtained from the first integral in Eq. (20), when evaluated at the outlet of the pipe, $X = L$, where mass exits the system:

$$\left. \frac{\partial T'}{\partial \dot{q}_i} \right|_{X=L} = \rho_F \left(\dot{u}_L + U(1+u'_L) \right) \frac{\partial \dot{u}_L}{\partial \dot{q}_i} + \rho_F \left(\dot{w}_L + Uw'_L \right) \frac{\partial \dot{w}_L}{\partial \dot{q}_i}, \tag{34}$$

see Eq. (28). The first surface integral in Eq. (20) evaluated at the outlet of the pipe then reads

$$\int_{A_L} \mathrm{d}\mathbf{a}\cdot(\mathbf{v}_F-\mathbf{v}_P)\frac{\partial T'}{\partial \dot{q}_i}=A_L\boldsymbol{\tau}_L\cdot U\boldsymbol{\tau}_L\frac{\partial T'}{\partial \dot{q}_i}\bigg|_{x=L}=A_L U\|\boldsymbol{\tau}_L\|^2\frac{\partial T'}{\partial \dot{q}_i}\bigg|_{x=L}=A_L U\frac{\partial T'}{\partial \dot{q}_i}\bigg|_{x=L} \tag{35}$$

and after having substituted Eq. (34), follows

$$\int_{A_L} \mathrm{d}\mathbf{a}\cdot(\mathbf{v}_F-\mathbf{v}_P)\frac{\partial T'}{\partial \dot{q}_i}=MU\left(\dot{u}_L\frac{\partial \dot{u}_L}{\partial \dot{q}_i}+\dot{w}_L\frac{\partial \dot{w}_L}{\partial \dot{q}_i}\right)+MU^2\left(\left(1+u'_L\right)\frac{\partial \dot{u}_L}{\partial \dot{q}_i}+w'_L\frac{\partial \dot{w}_L}{\partial \dot{q}_i}\right). \tag{36}$$

The inextensibility condition of Eq. (9) can be transformed into

$$(1+u')\frac{\partial u'}{\partial q_i}+w'\frac{\partial w'}{\partial q_i}=0 \tag{37}$$

and when applied to Eq. (25), renders

$$\frac{\partial T_F}{\partial q_i}=MU\int_0^L\left(\dot{u}\frac{\partial u'}{\partial q_i}+\dot{w}\frac{\partial w'}{\partial q_i}\right)\mathrm{d}X. \tag{38}$$

Integration by parts of Eq. (38) yields

$$\begin{aligned}\frac{\partial T_F}{\partial q_i}&=MU\int_0^L\left(\dot{u}\frac{\partial u'}{\partial q_i}+\dot{w}\frac{\partial w'}{\partial q_i}\right)\mathrm{d}X\\&=MU\left[\dot{u}\frac{\partial u}{\partial q_i}\right]_0^L-MU\int_0^L\dot{u}'\frac{\partial u}{\partial q_i}\,\mathrm{d}X+MU\left[\dot{w}\frac{\partial w}{\partial q_i}\right]_0^L-MU\int_0^L\dot{w}'\frac{\partial w}{\partial q_i}\,\mathrm{d}X.\end{aligned} \tag{39}$$

Comparison of Eqs. (39) and (36) leads to

$$\int_{A_L} \mathrm{d}\mathbf{a}\cdot(\mathbf{v}_F-\mathbf{v}_P)\frac{\partial T'}{\partial \dot{q}_i}-\frac{\partial T_F}{\partial q_i}=MU^2\left(\left(1+u'_L\right)\frac{\partial \dot{u}_L}{\partial \dot{q}_i}+w'_L\frac{\partial \dot{w}_L}{\partial \dot{q}_i}\right)-MU\int_0^L\left(\dot{u}'\frac{\partial u}{\partial q_i}+\dot{w}'\frac{\partial w}{\partial q_i}\right)\mathrm{d}X. \tag{40}$$

Inserting Eq. (18) into Eq. (26) yields the generalized forces due to gravity and elastic deformation of the pipe system

$$Q_i=-\frac{\partial V}{\partial q_i}=g(m+M)\int_0^L\frac{\partial u}{\partial q_i}\,\mathrm{d}X-\mathrm{EI}\int_0^L\left(\frac{w''}{1-w'^2}\frac{\partial w''}{\partial q_i}+\frac{w'w''^2}{\left(1-w'^2\right)^2}\frac{\partial w'}{\partial q_i}\right)\mathrm{d}X. \tag{41}$$

After two consecutive integrations by parts of the second integral in Eq. (41), taking the boundary conditions of the pipe system into account, one obtains

$$\begin{aligned}Q_i&=g(m+M)\int_0^L\frac{\partial u}{\partial q_i}\,\mathrm{d}X-\mathrm{EI}\int_0^L\left(\frac{\partial^2}{\partial X^2}\frac{w''}{1-w'^2}-\frac{\partial}{\partial X}\frac{w'w''^2}{\left(1-w'^2\right)^2}\right)\frac{\partial w}{\partial q_i}\,\mathrm{d}X\\&=g(m+M)\int_0^L\frac{\partial u}{\partial q_i}\,\mathrm{d}X-\mathrm{EI}\int_0^L\left(\frac{w^{(IV)}}{1-w'^2}+\frac{w''^3+4w'w''w'''}{\left(1-w'^2\right)^2}+\frac{4w'^2w''^3}{\left(1-w'^2\right)^3}\right)\frac{\partial w}{\partial q_i}\,\mathrm{d}X.\end{aligned} \tag{42}$$

Moreover, introducing the so-called Helmholtz auxiliary equations [24],

$$\frac{\partial u}{\partial q_i}=\frac{\partial \dot{u}}{\partial \dot{q}_i},\quad \frac{\partial w}{\partial q_i}=\frac{\partial \dot{w}}{\partial \dot{q}_i} \tag{43}$$

and inserting Eqs. (22), (23), (40) and (42) into Eq. (20) yields the nonlinear equations of motion for a cantilever elastica pipe with internal flow

$$(m+M)\int_0^L\left(\ddot{u}\frac{\partial u}{\partial q_i}+\ddot{w}\frac{\partial w}{\partial q_i}\right)\mathrm{d}X+2MU\int_0^L\left(\dot{u}'\frac{\partial u}{\partial q_i}+\dot{w}'\frac{\partial w}{\partial q_i}\right)\mathrm{d}X$$
$$+MU^2\left((1+u'_L)\frac{\partial u_L}{\partial q_i}+w'_L\frac{\partial w_L}{\partial q_i}\right)-g(m+M)\int_0^L\frac{\partial u}{\partial q_i}\,\mathrm{d}X$$
$$+\mathrm{EI}\int_0^L\left(\frac{w^{(IV)}}{1-w'^2}+\frac{w''^3+4w'w''w'''}{\left(1-w'^2\right)^2}+\frac{4w'^2w''^3}{\left(1-w'^2\right)^3}\right)\frac{\partial w}{\partial q_i}\,\mathrm{d}X=0. \tag{44}$$

By means of the following dimensionless parameters:

$$\xi=\frac{X}{L},\quad \upsilon=\frac{u}{L},\quad \eta=\frac{w}{L},\quad \tau=t\frac{1}{L^2}\sqrt{\frac{\mathrm{EI}}{m+M}},\quad \hat{U}=UL\sqrt{\frac{M}{\mathrm{EI}}},\quad \gamma=gL^3\frac{m+M}{\mathrm{EI}},\quad \beta=\frac{M}{m+M}, \tag{45}$$

the nonlinear equations of motion from Eq. (44) can be written in dimensionless form as

$$\int_0^1\left(\ddot{\upsilon}\frac{\partial\upsilon}{\partial q_i}+\ddot{\eta}\frac{\partial\eta}{\partial q_i}\right)\mathrm{d}\xi+2\sqrt{\beta}\hat{U}\int_0^1\left(\dot{\upsilon}'\frac{\partial\upsilon}{\partial q_i}+\dot{\eta}'\frac{\partial\eta}{\partial q_i}\right)\mathrm{d}\xi$$
$$+\int_0^1\left(\frac{\eta^{(\mathrm{IV})}}{1-\eta'^2}+\frac{\eta''^3+4\eta'\eta''\eta'''}{\left(1-\eta'^2\right)^2}+\frac{4\eta'^2\eta''^3}{\left(1-\eta'^2\right)^3}\right)\frac{\partial\eta}{\partial q_i}\,\mathrm{d}\xi$$
$$+\hat{U}^2\left((1+\upsilon'_L)\frac{\partial\upsilon_L}{\partial q_i}+\eta'_L\frac{\partial\eta_L}{\partial q_i}\right)-\gamma\int_0^1\frac{\partial\upsilon}{\partial q_i}\,\mathrm{d}\xi=0. \tag{46}$$

The weak form of the resulting equations of motion in Eq. (46) is perfectly suited to discretize in space by means of standard Ritz or similar methods. It will be shown in the following sections, that the inextensibility condition, Eq. (9), can be used to eliminate the axial displacement v from the equations of motion, resulting in similar equations as known from the literature. However, one of the advantages of the present form is a fully weak-form representation whereas existing equations, e.g. by Troger and Steindl [10, p. 372, Eqs. (L.22) and (L.25)], are given in an integro-differential form when incorporating the inextensibility condition.

4. Dimensional reduction

In this section, a dimensional reduction is proposed for the investigated elastica pipe system, stated in Eq. (46). The reduction process is based on the inextensibility condition from Eq. (9) and provides the possibility to deduce a minimum set of generalized coordinates describing the motion of this system. Eq. (9) is utilized for setting up a relation between u and w. Using the dimensionless parameters from Eq. (45) it follows that

$$\upsilon=\int_0^\xi\left(-1+\sqrt{1-\eta'^2}\right)\mathrm{d}\zeta. \tag{47}$$

The spatial integral in Eq. (47) is now solved by application of the Gauss–Legendre formula of order n given by

$$\int_a^b f(x)\,\mathrm{d}x=\int_{-1}^1 f\left(\frac{b-a}{2}\bar{\xi}+\frac{b+a}{2}\right)\left(\frac{b-a}{2}\,\mathrm{d}\bar{\xi}\right)=\frac{b-a}{2}\sum_{k=1}^n w(\bar{\xi}_k)\,g(\bar{\xi}_k)+R_n(\bar{\xi}), \tag{48}$$

see [25, p. 219] with $\bar{\xi}=(2x-b-a)/(b-a)$ and $\bar{\xi}_k$ denoting the kth zero of the Legendre polynomial $P_n(\bar{\xi})$ of the first kind. The weighting function $w(\bar{\xi}_k)$, the transformed integrand $g(\bar{\xi}_k)$ and the residuum $R_n(\bar{\xi})$ in

Eq. (48) can be computed as

$$w(\bar{\xi}_k) = \frac{2}{\left(1-\bar{\xi}_k^2\right)\left[P_n'(\bar{\xi}_k)\right]^2}, \quad g(\bar{\xi}) = f\left(\frac{b-a}{2}\bar{\xi}_k + \frac{b+a}{2}\right), \quad R_n(\bar{\xi}) = \frac{2^{2n+1}(n!)^4}{(2n+1)[(2n)!]^3} g^{(2n)}(\bar{\xi}). \tag{49}$$

A dimensional reduction utilizing the inextensibility condition, but restricted to low-order expressions of a Taylor-series expansion has been performed by Semler et al. [2]. Several other forms of dimensional reductions can be found in the literature, e.g. the center manifold reduction [26,27], where the dimension of a system of ordinary differential equations is reduced in the neighborhood of an equilibrium point. A second possible reduction method is the Lyapunov–Schmidt reduction (see e.g. [1, Appendix F]), that replaces the original set of PDEs with a reduced set of equations, which contains all essential information for a stability analysis.

5. Comparison to existing formulations

In this section, the equations of motion, deduced in Section 3, will be compared with formulations from the literature. First, the nonlinear equations of motion from Eq. (44) will be compared with the nonlinear equations presented by Folley and Bajaj [9] and Troger and Steindl [10]. In the derivations of these works, no approximations or order-of-magnitude considerations were preformed and a geometrical exact formulation for the curvature was applied. The comparison will be performed on a term-by-term basis. Second, the equations of motion deduced in the present work will be compared with the equations of motion for cantilever pipe systems, presented by Semler and Païdoussis [1,2]. The derivation of the latter equations includes order-of-magnitude considerations of the cantilever pipe system. Numerical solutions for varying system parameters will be shown.

5.1. Comparison to Folley and Bajaj's equations, Ref. [9]

The equations of motion presented by Folley and Bajaj [9] are based on a Newtonian approach for an infinitesimal tube element. A three-dimensional model of a cantilevered tube is considered. Since the pipe system investigated in this paper is restricted to plane motions, the y direction in the model of Bajaj [9, p. 16], is set to $y = 0$, resulting in the fact that the unit vector $\mathbf{t}_2 = \mathbf{0}$ in Ref. [9, Eq. (2.5)] and hence also the twist of the tube $\tau = 0$. The basic assumptions for the tube are coinciding with the assumptions in this work, with the exception, that we do not consider dissipative terms in the derivation of the equations of motion and therefore the damping coefficient χ of [9] needs to be set to $\chi = 0$ in order to compare the resulting equations. The assumptions made for the fluid are coinciding with the assumptions made here. In the first step of the derivation, the moment balance is written to obtain the axial load acting on the tube segment. In a second step, the force balance for a small tube segment is written to obtain the equations of motion. The final equation of motion is represented in Ref. [9, Eq. (2.25)] for the transverse displacement u and the axial displacement w, which corresponds to u and w in the present paper. Incorporating all assumptions as stated above [9 (2.25)] follows

$$(m+M)\ddot{u} + 2MU\dot{u}' + MU^2u'' + \mathrm{EI}\,u^{(IV)} = u''(u'\ddot{u}'' + w'\ddot{w}'') + \left((N - P - \mathrm{EI}\,\kappa^2)u'\right)' \tag{50}$$

with the axial load

$$N - P + \frac{1}{2}\mathrm{EI}\,\kappa^2 = \left(N - P + \frac{1}{2}\mathrm{EI}\,\kappa^2\right)_{X=L} + (m+M)g\int_X^L w'\,\mathrm{d}\xi - (m+M)\int_X^L (u'\ddot{u} + w'\ddot{w})\,\mathrm{d}\xi. \tag{51}$$

Direct transformation of the equations of motion presented above in Eq. (44) into the form of Folley and Bajaj shown in Eqs. (50) and (51) is possible, but tedious, as pointed out by Païdoussis in Ref. [1, p. 503]. However, terms characterizing the dynamics of the system in the equations of motion can be compared. The first expression in Eq. (44) denotes the elements of the mass matrix of the system presented here. These terms, as stated in Ref. [9, p. 22], can be identified in Eq. (50) when inserting the axial load from Eq. (51). The second expression in Eq. (44) includes the mixed derivatives of the axial and transverse deflections corresponding to the coriolis forces in the pipe system and can also be identified in Eq. (50). The third term in Eq. (44) denotes

the centrifugal force expressions including the square of fluid velocity U and can be transformed into the form of Eq. (50) using the inextensibility condition from Eq. (9), as shown in Ref. [1, p. 285]. The fourth term in Eq. (44) includes the gravitational forces acting in the X direction of the inertial frame. The corresponding terms in the equations of Folley and Bajaj are included in the net axial load, Eq. (51). Again, application of the inextensibility condition, Eq. (9), to the gravitational term in Eq. (44) yields the form of the corresponding expression in Eq. (51). The last expression in the equations of motion includes the expressions for the potential energy due to elastic deformation of the pipe. In order to compare the resulting terms to the work of Folley and Bajaj [9], several steps utilizing Frenet's formulas for a local material coordinate system, as introduced in Ref. [9, p. 16] are required. The transformation of the expressions due to elastic deformation presented here to the expressions of Folley and Bajaj, based on the curvature κ of the pipe, is given in Appendix A. Summarizing the term-by-term comparison, it follows that, for coinciding material parameters of the investigated system, all expressions in the equations of motion presented here can be identified in the equations of Folley and Bajaj, Eqs. (50) and (51).

Folley and Bajaj showed in their work [9] the behavior of the linearized cantilevered pipe system [9, p. 36, Eq. 3.12] by means of an eigenvalue analysis [9, p. 36, Fig. 4]. In order to compare the results of a linear analysis for varying system parameters, the inextensibility condition, Eq. (9), is inserted into the equations of motion, Eq. (44), and linearized about the static equilibrium position $w = 0$, and an eigenvalue analysis is performed afterwards. The linearized equation of motion can be written in the following way (see also [1, Chapter 1]):

$$\mathbf{M}\,\ddot{\mathbf{q}} + \mathbf{C}\,\dot{\mathbf{q}} + \mathbf{K}\,\dot{\mathbf{q}} = \mathbf{Q} \tag{52}$$

with $\mathbf{M}$ denoting mass matrix, $\mathbf{C}$ and $\mathbf{K}$ are the damping and the stiffness matrix, respectively. The generalized forces are combined in the vector $\mathbf{Q}$. In the next step, the system is transformed to its first-order form

$$\mathbf{B}\,\dot{\mathbf{z}} + \mathbf{E}\,\mathbf{z} = \mathbf{\Phi} \tag{53}$$

with the following elements:

$$\mathbf{B} = \begin{bmatrix} \mathbf{0} & \mathbf{M} \\ \mathbf{M} & \mathbf{C} \end{bmatrix}, \quad \mathbf{E} = \begin{bmatrix} -\mathbf{M} & \mathbf{0} \\ \mathbf{0} & \mathbf{K} \end{bmatrix}, \quad \mathbf{\Phi} = \begin{bmatrix} \mathbf{0} \\ \mathbf{Q} \end{bmatrix} \quad \mathbf{z} = \begin{bmatrix} \dot{\mathbf{q}} \\ \mathbf{q} \end{bmatrix}. \tag{54}$$

Solutions of the form $\mathbf{z} = \mathbf{A}\,\mathrm{e}^{\lambda t}$ lead to the following eigenvalue problem:

$$(\lambda\mathbf{I} - \mathbf{Y})\mathbf{A} = 0, \tag{55}$$

where $\mathbf{A}$ denotes the eigenvectors and λ the corresponding eigenvalues of the system. Using the matrices $\mathbf{B}$ and $\mathbf{E}$, the matrix $\mathbf{Y}$ follows

$$\mathbf{Y} = -\mathbf{B}^{-1}\mathbf{E}. \tag{56}$$

The Argand diagram for the eigenvalues of the linearized equations of motion, for a mass ratio $\beta = 0.6$ and varying fluid velocity U, is shown in Fig. 3. Comparing the results to Folley and Bajaj [9, p. 40], the solution of the linearized form of the equations of motion of the present paper shows coinciding behavior in the framework of a linear stability theory. In full agreement with the solutions presented by Folley and Bajaj [9, p. 40, Fig. 4], the system loses stability in its second mode at a critical flow velocity of $\hat{U} = 9.8$.

After comparing the linearized equations of motion, a numerical nonlinear analysis of the equation of motion, Eq. (44), is compared with the results of Folley and Bajaj [9]. As pointed out by Folley and Bajaj in Ref. [9, p. 52], the dynamical pipe behavior depends on two parameters, the fluid velocity U and the mass ratio β. In Fig. 4, the graph of a numerical study for the critical flow velocity, being the flow velocity U where the system first enters an unstable state, vs. the mass ratio β is shown. In comparison to the results presented in Ref. [9, p. 51, Fig. 5], all characterizing parts of the graph can also be found in the results shown in Fig. 4. For a mass ratio β in the vicinity of 0.3, the graph shows multiple possible values of the critical flow velocity. A similar effect can be found for β near 0.7 also.

The equations of motion deduced in Troger and Steindl [10, Appendix L] are mainly based on the work by Lundgren et al. [11], extending the latter work by including damping and gravitational effects, as well as a rotationally symmetric elastic support of the tube. The derivation of the equations of motion is basically

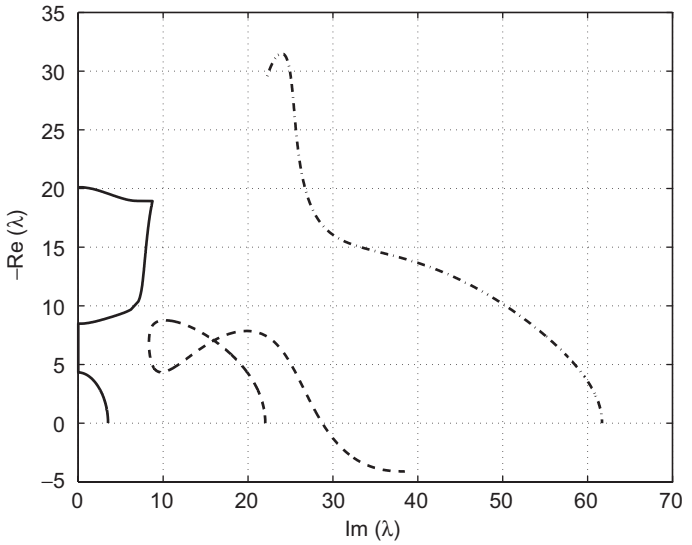

Fig. 3. Argand diagram of the eigenvalues of the three lowest modes as a function of U. —— 1st mode, - - - - - - 2nd mode and – · – · – 3rd mode.

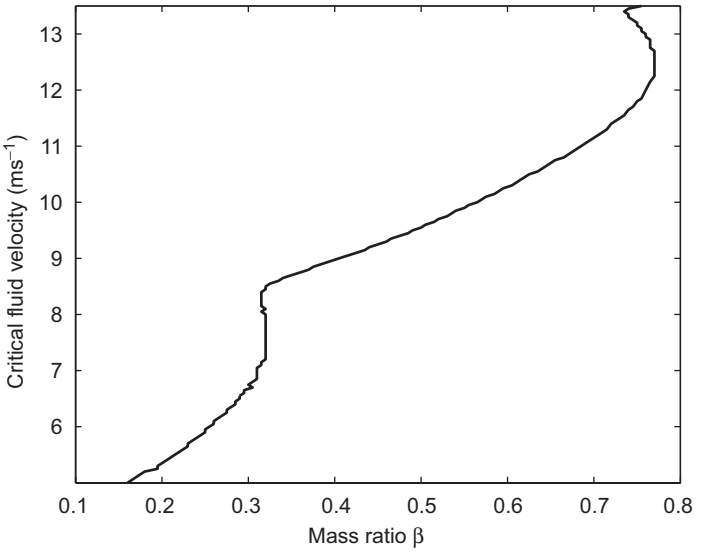

Fig. 4. Critical fluid velocity as a function of the mass ratio β.

conforming to the work of Folley and Bajaj [9], with two differences. First, it is assumed that no axial torque is acting on the tube and therefore the twist τ is set to zero when deriving the final equations of motion. Second, the integration of the net axial load [10, Eq. (L.22)] is split into two parts to be able to include an elastic intermediate or end support acting on the tube. Owing to the fact that Eq. (44) are based on planar motions with no intermediate or end supports, the equations of Troger and Steindl [10] and Folley and Bajaj [9] reduce to the same set of equations shown in Eqs. (50) and (51).

5.2. Comparison to Semler and Païdoussis' equations, Refs. [1,2]

In the following, the PDEs of Semler and Païdoussis [1,2] will be compared with lower-order versions of the equations deduced in the present work. In order to obtain the solutions for small pipe deflections out of the

nonlinear equation of motion, Eq. (46), the square root in Eq. (47) is transformed into a binomial series resulting in

$$\upsilon = -\xi + \int_0^{\xi} \sum_{n=1}^{\infty} (-1)^{n-1} \binom{\frac{1}{2}}{n-1} \eta'^{2n-2} \, \mathrm{d}\zeta. \tag{57}$$

The bracketed expression in Eq. (57) denotes the binomial coefficient defined by

$$\binom{n}{k} = \frac{n!}{k!(n-k)!}. \tag{58}$$

The binomial series, evaluated for a limited set of coefficients, $n = 3$, yields

$$\upsilon = -\xi + \int_0^{\xi} \sum_{n=1}^{3} (-1)^{n-1} \binom{\frac{1}{2}}{n-1} \eta'^{2n-2} \, \mathrm{d}\zeta = -\int_0^{\xi} \left(\frac{1}{2}\eta'^2 + \frac{1}{8}\eta'^4 \right) \mathrm{d}\zeta. \tag{59}$$

The next approximation in the reference equations [1,2] is made in the formulation for the strain energy expression of the pipe. The potential energy is obtained applying a truncated Taylor series of the curvature expression for an inextensible beam axis of a Bernoulli–Euler beam. In order to obtain this expression from the potential energy due to elastic deformation, stated in Eq. (18), the following approximation has to be performed:

$$V_d = \frac{1}{2} \mathrm{EI} \int_0^L \frac{w''^2}{1 - w'^2} \, \mathrm{d}X \approx \frac{1}{2} \mathrm{EI} \int_0^L w''^2 \left(1 + w'^2 \right) \mathrm{d}X. \tag{60}$$

The corresponding generalized forces Q_i, including gravitational effects, follow

$$Q_i = -\frac{\partial V}{\partial q_i} = g(m+M) \int_0^L \frac{\partial u}{\partial q_i} \, \mathrm{d}X - \mathrm{EI} \int_0^L \left(w'' \left(1 + w'^2 \right) \frac{\partial w''}{\partial q_i} + w' w''^2 \frac{\partial w'}{\partial q_i} \right) \mathrm{d}X. \tag{61}$$

Partial integration of Eq. (61) yields

$$Q_i = g(m+M) \int_0^L \frac{\partial u}{\partial q_i} \, \mathrm{d}X - \mathrm{EI} \int_0^L \left(w^{(IV)} \left(1 + w'^2 \right) + 4 w' w'' w''' + w''^3 \right) \frac{\partial w}{\partial q_i} \, \mathrm{d}X. \tag{62}$$

Introducing the dimensionless parameters from Eq. (45) gives

$$Q_i = \gamma \int_0^1 \frac{\partial \upsilon}{\partial q_i} \, \mathrm{d}\xi - \int_0^1 \left(\eta^{(IV)} \left(1 + \eta'^2 \right) + 4 \eta' \eta'' \eta''' + \eta''^3 \right) \frac{\partial \eta}{\partial q_i} \, \mathrm{d}\xi. \tag{63}$$

In order to find the corresponding form of equations of motion as given in the reference equations [1,2], the nonlinear equations of motion in dimensionless form written in Eq. (46) need to be evaluated for the truncated dimensionless displacement υ in Eq. (59). The corresponding derivative of υ in the equations of motion from Eq. (46) follows

$$\ddot{\upsilon} = -\int_0^{\xi} \left(\dot{\eta}'^2 \left(1 + \frac{3}{2}\eta'^2 \right) + \ddot{\eta}' \left(\eta' + \frac{1}{2}\eta'^3 \right) \right) \mathrm{d}\zeta \approx -\int_0^{\xi} \left(\dot{\eta}'^2 + \ddot{\eta}' \eta' \right) \mathrm{d}\zeta, \tag{64}$$

$$\dot{\upsilon}' = -\int_0^{\xi} \left(\dot{\eta}' \eta'' \left(1 + \frac{3}{2}\eta'^2 \right) + \dot{\eta}'' \eta' \left(1 + \frac{1}{2}\eta'^2 \right) \right) \mathrm{d}\zeta \approx -\int_0^{\xi} \left(\dot{\eta}' \eta'' + \dot{\eta}'' \eta' \right) \mathrm{d}\zeta, \tag{65}$$

$$\frac{\partial \upsilon}{\partial q_i} = -\int_0^{\xi} \eta' \left(1 + \frac{1}{2}\eta'^2 \right) \frac{\partial \eta'}{\partial q_i} \, \mathrm{d}\zeta = -\eta' \left(1 + \frac{1}{2}\eta'^2 \right) \frac{\partial \eta}{\partial q_i} + \int_0^{\xi} \eta'' \left(1 + \frac{3}{2}\eta'^2 \right) \frac{\partial \eta'}{\partial q_i} \, \mathrm{d}\zeta. \tag{66}$$

In Eqs. (64) and (65), further order-of-magnitude considerations are to be performed, limiting the dimensionless transverse displacement η to terms smaller than order 4. Now equations of the same order as the reference equation [1, Eq. (5.39)], can be written substituting Eqs. (64)–(66) into the nonlinear equations of motion, Eq. (46).

The resulting equations of motion agree with the equations presented by Semler and Païdoussis [1,2]. In order to write the equations in the same form as presented here, a Galerkin method has to be applied to the PDE of motion [1, Eq. 5.39]. The effects of the order-of-magnitude truncations, necessary to obtain the equations of Semler and Païdoussis, on large pipe deformations will be discussed in the numerical examples presented in Section 7.

The latter derivations complete this section devoted to the comparison of the present equations to previously published equations of motion in the literature. In the following section, a discrete mass formulation, allowing a continuous movement of one or more discrete masses with large deformations of the pipe, will be introduced.

6. Comparison with discrete mass formulation

The solution of the coupled pipe and fluid problem with a higher-order Euler elastica is not yet available in the literature. Therefore, the solution of the presented formulation is compared with an existing software program that can compute the dynamic behavior of large deformation beam elements and rigid bodies. A good approximation of the idealized pipe flow is gained through an approximation with many discrete masses that are distributed along the beam axis. The masses move with the velocity of the fluid and have the same mass per length as the fluid.

The multibody software HOTINT/MBS is used to model the nonlinear deformation of the cantilever beam by means of the so-called absolute nodal coordinate formulation [21]. A planar third-order beam element similar to the one derived by Gerstmayr and Shabana [28] is utilized, see Fig. 5. The position $\mathbf{r}$ of the beam is approximated by the deformation field vs. the axial coordinate X by means of

$$\mathbf{r} = \begin{bmatrix} a_0 + a_1 X + a_2 X^2 + a_3 X^3 \\ b_0 + b_1 X + b_2 X^2 + b_3 X^3 \end{bmatrix}. \tag{67}$$

The parameters a_i are unknown coefficients which are usually transformed into nodal coordinates [28]. The equations of motion are gained from D'Alembert's principle written for the volume V of the beam element [28],

$$\int_V \rho\, \ddot{\mathbf{r}}^{\mathrm{T}} \delta\mathbf{r}\, \mathrm{d}V + \int_V \mathbf{S} : \delta\mathbf{E}\, \mathrm{d}V = \int_V \mathbf{f}_{\mathrm{ext}}^{\mathrm{T}}\, \delta\mathbf{r}\, \mathrm{d}V, \tag{68}$$

where ρ denotes the mass density of the beam, $\mathbf{S}$ is the second Piola Kirchhoff stress tensor, $\mathbf{E}$ is the fully nonlinear Green strain tensor and $\mathbf{f}_{\mathrm{ext}}$ represents external forces, and forces resulting from Lagrange multipliers. The discrete masses are modeled by single mass points of mass m, obeying the equations of motion for the displacement u,

$$\begin{bmatrix} m & 0 \\ 0 & m \end{bmatrix} \begin{bmatrix} \ddot{u}_X \\ \ddot{u}_Y \end{bmatrix} = \begin{bmatrix} F_X \\ F_Y \end{bmatrix}, \tag{69}$$

where F_X and F_Y are forces applied to the mass. The interaction of the nonlinear beam and the mass points are taken into account by constraint equations. A so-called sliding joint that is usually available in multibody simulation software, allows a point of one body to move along the surface of another body, see Fig. 5.

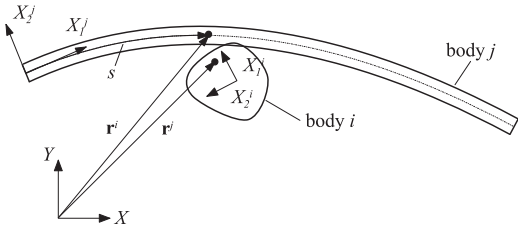

Fig. 5. Absolute nodal coordinate formulation beam element and sliding parameter s.

Generally, it is assumed that a fixed point $\mathbf{x}^i$ of the flexible or rigid body i is sliding along the centerline of a beam denoted as body j. The local (undeformed) positions of the sliding point on body i and j are given by

$$\mathbf{x}^i = \begin{pmatrix} X_1^i \\ X_2^i \end{pmatrix} \quad \text{and} \quad \mathbf{x}^j = \begin{pmatrix} X_1^j = s \\ 0 \end{pmatrix}, \tag{70}$$

where s represents the sliding parameter with respect to the beam axis. Note that in the present case of discrete mass points the vector $\mathbf{x}^i = [0\ 0]^{\mathrm{T}}$ coincides with the center of mass. The following constraint equations must be fulfilled for the sliding joint

$$\mathbf{C} = \begin{bmatrix} \mathbf{r}^i(X_1^i,\ X_2^i) - \mathbf{r}^j(s) \\ \dfrac{\partial \mathbf{r}^j(s)}{\partial s} \cdot \boldsymbol{\lambda} \end{bmatrix} = \mathbf{0}. \tag{71}$$

In Eq. (71), the first line is used to restrict the motion of the sliding point on body i and j to be at the same global position. This leads to two Lagrange multipliers $\boldsymbol{\lambda} = [\lambda_1 \quad \lambda_2]^{\mathrm{T}}$ associated with the constraint forces applied to both bodies. The vector of Lagrange multipliers must be perpendicular to the sliding direction, which means, that in the friction-free case there is no force acting in the sliding direction. This is satisfied by means of the second line in Eq. (71). The sliding parameter s, which is a non-generalized coordinate of the sliding joint, can be systematically eliminated. The sliding parameter s can be determined by using the equation

$$\left(\mathbf{r}^i(X_1^i,\ X_2^i) - \mathbf{r}^j(s)\right)^{\mathrm{T}} \frac{\partial \mathbf{r}^j(s)}{\partial s} = 0. \tag{72}$$

This equation constrains the points of the two bodies in the sliding direction and therefore results only in one equation, which is of order 3 in s and can be solved for the sliding parameter s by means of the Newton method.

7. Numerical results

In this section, the numerical solution of the equations of motion, Eq. (44), for the cantilever elastica pipe shown in Fig. 1, is compared with the solution of Païdoussis [1, Eq. (5.28)] and to the discrete mass formulation presented in the previous section. The material parameters are $m = 8\,\mathrm{kg\,m^{-1}}$, $M = 2\,\mathrm{kg\,m^{-1}}$, $L = 1\,\mathrm{m}$ and $\mathrm{EI} = 10\,\mathrm{N\,m^2}$. Eq. (44) is solved applying a 5-mode Ritz–Ansatz for the transverse deflection w. In a recent study [29], it could be shown that 5 modes provide converged and coinciding results with a finite element approach. The axial displacement u is eliminated from Eq. (44) using Eq. (47) in combination with an order 17 Gaussian integration. Païdoussis' equation is solved using a 5-mode Galerkin approximation. Here, one major difference to existing formulations appears. The application of a Ritz method to the Lagrangian equations of motion, Eq. (44), directly results in a finite set of ordinary differential equations. Opposed to this, the nonlinear PDE in Ref. [1] (and also the equations of Folley and Bajaj [9] and Troger and Steindl [10]) requires significantly more computational effort due to the Galerkin approximation of the nonlinear PDE of motion. The solutions of Eq. (44) and the outcomes of Païdoussis' equation are compared with a system, in which the fluid is replaced by n_m point-masses equally distributed along the beam with mass MLn_m^{-1}, see Section 6 above. The point-masses move with constant velocity with respect to the beam axis, such that $\dot{s} = U$. The initial velocity of the point-masses is equal to the velocity of the fluid in tangential direction of the beam axis at the support. During the simulation, the inflow and outflow of masses is taken into account, such that the distance between each mass is always Ln_m^{-1}, and, as soon as the first mass moves further than Ln_m^{-1} from the support, a new mass is introduced with initial velocity of the fluid. Fig. 6 shows the maximum amplitude of the tip of the cantilever between 4 and 6 s vs. the velocity of the masses and the fluid, respectively. The solutions of Eq. (44) and discrete mass formulation for varying fluid velocity U show very good agreement. The solutions of Païdoussis' equation [1, Eq. (5.28)] show good agreement for fluid velocities U smaller than $12.8\,\mathrm{m\,s^{-1}}$. For higher fluid velocities, where the deformation of the pipe increases, a significant difference can be observed, because the present derivation, based on geometrically exact elastica theory, provides better

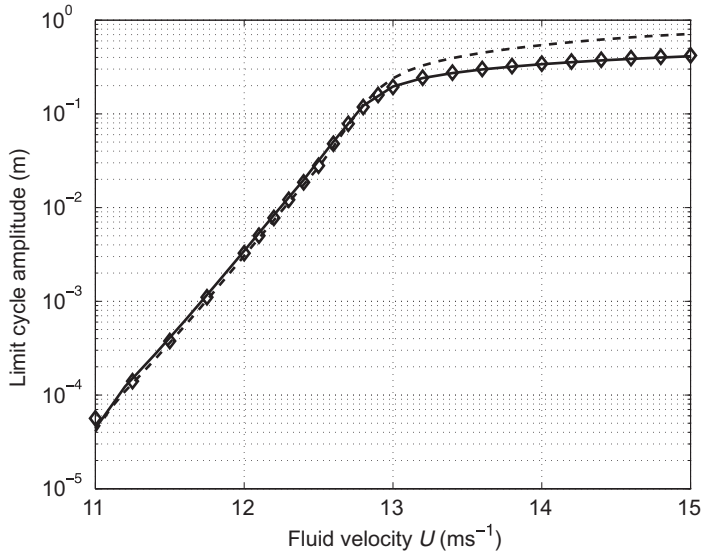

Fig. 6. Limit cycle amplitude of the pipe system as a function of U. —— Extended Lagrange formulation, ------ Païdoussis' equation [3] and ◇ discrete mass formulation.

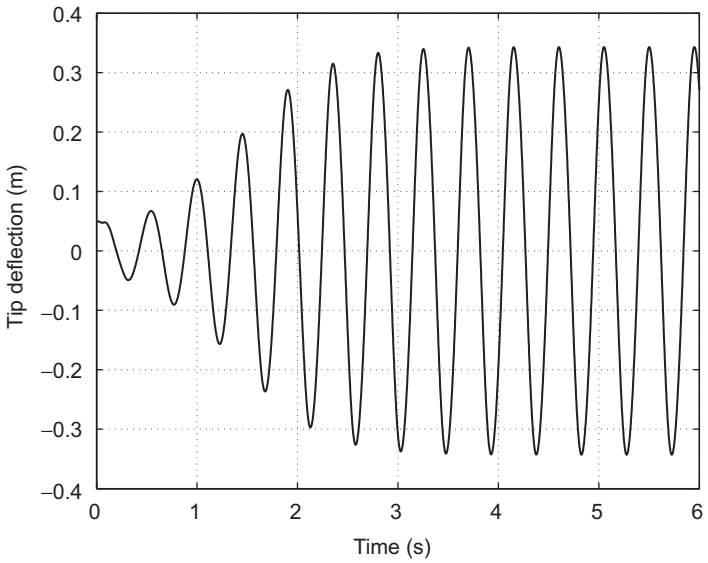

Fig. 7. Tip deflection for the case of 40 discrete masses with a velocity of 14 m s^{-1}.

results than scaled equations, in which order-of-magnitude consideration have been performed during derivation. Fig. 7 shows the tip deflection of the cantilever beam for the discrete mass simulation with 40 masses and a velocity of the masses of 14 m s^{-1}. The flutter instability reaches its maximum amplitude after 3 s of the simulation. Several deformed shapes of the cantilever problem are presented in Fig. 8 according to the tip deflection in Fig. 7.

As a further comparison of Eq. (46) and the formulation with discrete masses, Fig. 9 shows the maximum amplitude of the tip deflection between 4 and 6 s of the system with one, four and eight masses per beam length compared with the previously shown 40 masses. While the phenomenon of moving masses along a cantilever beam has been already studied in the literature, see e.g. [30], the solution and stability of the repeated

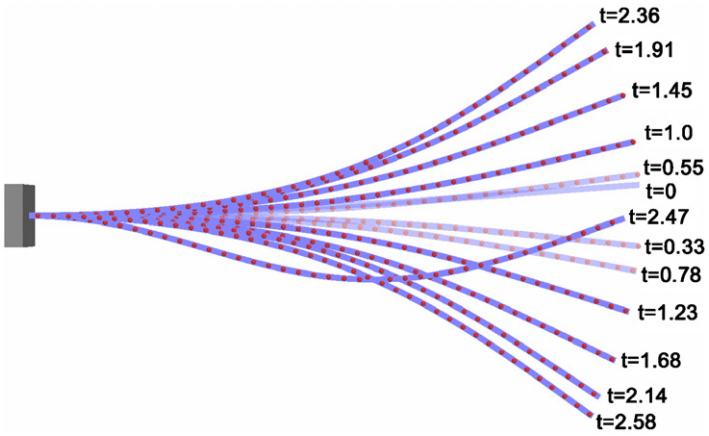

Fig. 8. Deformation shapes at different time instances during the simulation, according to the tip deflection presented in Fig. 7.

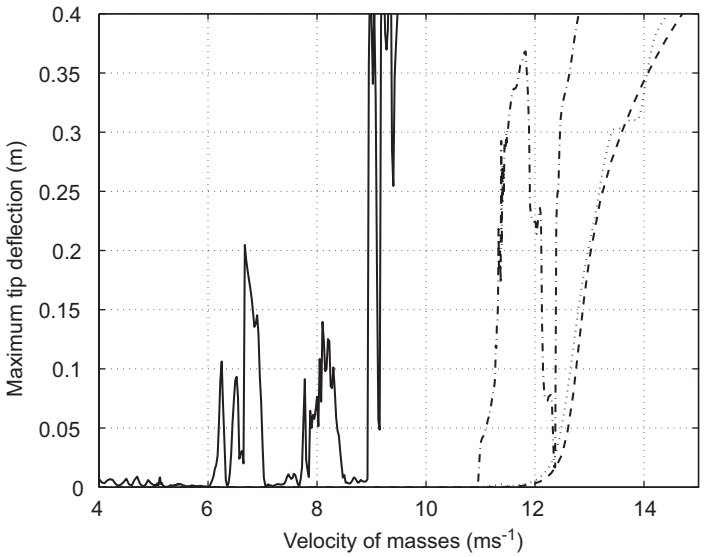

Fig. 9. Comparison of maximum tip deflection between 4 and 6 s for different numbers of discrete masses. —— 1 mass, – · – · – 4 masses, ... 8 masses and - - - - - - 40 masses.

movement of one or more masses along a beam is an open problem. Fig. 9 shows that the solution for a higher number of masses converges to the solution of the fluid problem. However, with a small number of masses, further instability phenomena occur in addition to the critical velocity of the fluid. In the case of one mass repeatedly moving along the beam, several instabilities are present at comparably small ranges of velocities. The first instability appears at about half the critical velocity of the fluid at $U = 6\,\mathrm{m\,s^{-1}}$, significant unstable regions are present around 6.7 and $8\,\mathrm{m\,s^{-1}}$, while above $8.9\,\mathrm{m\,s^{-1}}$ the system becomes unstable. It shall be mentioned, that Fig. 9 in fact only shows the deflection due to the excitation by the moving masses. While the method with discrete masses appeared to be suitable for the case of fluid problems, compare the previous sections, it might be interesting to further investigate the instability of single moving masses for a longer simulation time (e.g. to check the maximum amplitude after 50 s). In the case of four masses, the system becomes unstable by flutter at $11\,\mathrm{m\,s^{-1}}$, which is close to the third eigenfrequency of the cantilever beam without fluid, while in the case of eight masses, the discrete mass solution almost coincides with the solution obtained for the continuous system in Eq. (44) for 5 modes. The interpretation of the unstable domains for the solution with a small number of masses is difficult and is left to a further investigation. In principle, they may

be coupled either to the bending eigenfrequency or a multiple of it, or to the bending wave propagation, which has different wave speed for different frequency of the wave content.

8. Conclusions

A novel alternative approach for the analysis of nonlinear vibrations for pipe systems conveying fluids is presented. The example of a cantilever pipe modeled as a Euler elastica has been investigated. The proposed approach utilizes an extended version of the Lagrange equations for systems containing non-material volumes, where the equations of motion directly result in a finite set of ordinary differential equations. Order-of-magnitude assumptions are omitted in the derivation of the equations of motion, providing the possibility of studying large deformations of the considered system. For the resulting equations of motion, a dimensional reduction with arbitrary order of approximation was introduced. The resulting equations of motion were compared with previously published equations by Païdoussis [1], Folley and Bajaj [9] and Troger and Steindl [10]. First, the final nonlinear equations of motion were compared on a term-by-term basis. Owing to the fact, that the equations from the literature are all written in the form of a PDE, in contrast to the ordinary differential equations presented in this work, direct comparison is tedious. However, all characterizing terms in the previously published equations of motion by Folley and Bajaj [9] and Troger and Steindl [10], where exact curvature expressions without order-of-magnitude considerations have been performed, have been identified in the equations presented in this work. This leads to the second type of comparison in terms of a stability analysis, which has been performed for the linearized equations of motion in terms of an eigenvalue analysis, and for the full nonlinear equations in a numerical way for varying system parameters.

For the equations presented by Païdoussis [1], solutions of the resulting equations of motion [1, Eq. (5.28)] have been recomputed for varying system parameters in order to provide best comparability. As a result, it was shown, that the order-of-magnitude considerations performed by Païdoussis provide sufficient accuracy for small deflections of the pipe system. However, for larger amplitudes the full nonlinear equations of motion need to be considered in order to reproduce the present results and the results of a finite element approach with discrete masses and nonlinear behavior. Although the equations presented by Folley and Bajaj [9] and Troger and Steindl [10] include no simplifications or order-of-magnitude considerations, the computation of solutions demands a very high computational effort due to the form of a nonlinear PDE of motion for an infinitesimal pipe element. Even for the nonlinear equations presented by Païdoussis [1], including order-of-magnitude considerations, the computation time in comparison to the solution of the full nonlinear equations presented here is at least a factor ten higher.

The solution of the pipe conveying fluid has been compared with a second approach based on discrete masses that is available in the multibody code HOTINT/MBS. A large number of discrete masses were used to model the motion of the fluid moving along the axis of the beam, discretized by many nonlinear finite elements. The presented models showed very good agreement, both in the stable as well as the unstable regime. As a further result, the solution with a small number of discrete masses is presented that might be interesting for other transport problems or fluids containing gas bubbles, and it is planned to incorporate the Lagrange equation-based formulation of Eq. (44) into a multibody computer code in the near future.

Acknowledgments

Support of the authors by the peer-reviewed Kplus Linz Center of Mechatronics GmbH (LCM) and support of the author J. Gerstmayr by an APART scholarship of the Austrian Academy of Sciences (ÖAW) is gratefully acknowledged. The authors wish to thank Prof. Peter Paule, Research Institute for Symbolic Computation (RISC), Johannes Kepler University Linz, Austria, for his valuable comments.

Appendix A. Virtual work of a finite tube element

The moment balance for an infinitesimal small differential tube element [9, Eq. (2.15)] gives the relation

$$\mathbf{M}' + \boldsymbol{\tau} \times \mathbf{Q} = \mathbf{0}, \tag{73}$$

where $\mathbf{M}$ denotes the moment vector and $\mathbf{Q}$ the vector of the resultant forces. By taking the cross-product with the tangent unit vector τ yields

$$\mathbf{Q} = N\boldsymbol{\tau} + \boldsymbol{\tau} \times \mathbf{M}', \tag{74}$$

where N denotes the axial force acting on the tube element. The virtual work for a deformed pipe element can be written as

$$\begin{aligned}\delta W &= \int_0^L \mathbf{Q}' \cdot \delta\mathbf{r}_0 \,\mathrm{d}X = [\mathbf{Q}\delta\mathbf{r}_0]_0^L - \int_0^L \mathbf{Q} \cdot \delta\boldsymbol{\tau} \,\mathrm{d}X = -\int_0^L (N\boldsymbol{\tau}) \cdot \delta\boldsymbol{\tau} - \int_0^L (\boldsymbol{\tau} \times \mathbf{M}') \cdot \delta\boldsymbol{\tau} \\ &= -\int_0^L (N\boldsymbol{\tau}) \cdot \delta\boldsymbol{\tau} + \int_0^L \mathbf{M}' \cdot (\boldsymbol{\tau} \times \delta\boldsymbol{\tau}) = -\int_0^L (N\boldsymbol{\tau}) \cdot \delta\boldsymbol{\tau} + [\mathbf{M} \cdot (\boldsymbol{\tau} \times \delta\boldsymbol{\tau})]_0^L - \int_0^L \mathbf{M} \cdot (\boldsymbol{\tau} \times \delta\boldsymbol{\tau})' \\ &= -\int_0^L (N\boldsymbol{\tau}) \cdot \delta\boldsymbol{\tau} - \int_0^L \mathbf{M} \cdot (\boldsymbol{\tau}' \times \delta\boldsymbol{\tau} + \boldsymbol{\tau} \times \delta\boldsymbol{\tau}'). \end{aligned} \tag{75}$$

The binormal vector and its variation are introduced, using the tangent unit vector $\boldsymbol{\tau}$ from Eq. (11) and the normal unit vector $\mathbf{v}$, Eq. (3), and follows

$$\mathbf{b} = \boldsymbol{\tau} \times \mathbf{v}, \quad \delta\mathbf{b} = \delta\boldsymbol{\tau} \times \mathbf{v} + \boldsymbol{\tau} \times \delta\mathbf{v} = \mathbf{0}. \tag{76}$$

The variation of the binormal vector vanishes for planar motions. Application of Frenet's formulas gives the relations between the tangent unit vector $\boldsymbol{\tau}$, the normal unit vector $\boldsymbol{\nu}$ and their spatial derivatives along the beam coordinate X:

$$\boldsymbol{\tau}' = \kappa\mathbf{v}, \quad \mathbf{v}' = -\kappa\boldsymbol{\tau} + \tau\mathbf{b} = -\kappa\boldsymbol{\tau}, \tag{77}$$

where κ denotes the curvature of the pipe axis and τ denotes its twist. The twist τ vanishes for planar motions. Using Eq. (77), the variations of the tangent unit vector and the normal unit vector can be computed by

$$\delta\boldsymbol{\tau} = \boldsymbol{\tau}'\delta X = \kappa\mathbf{v}\delta X, \quad \delta\mathbf{v} = \mathbf{v}'\delta X = -\kappa\boldsymbol{\tau}\delta X. \tag{78}$$

The virtual work δW, Eq. (75), can be rewritten by taking into account Eqs. (77) and (78) as

$$\begin{aligned}\delta W &= -\int_0^L (N\boldsymbol{\tau}) \cdot \delta\boldsymbol{\tau} - \int_0^L \mathbf{M} \cdot (\boldsymbol{\tau}' \times \delta\boldsymbol{\tau} + \boldsymbol{\tau} \times \delta\boldsymbol{\tau}') \\ &= -\int_0^L \underbrace{(N\boldsymbol{\tau}) \cdot \kappa\mathbf{v}}_{\tau \perp v \Rightarrow \tau \cdot v = 0} \delta X - \int_0^L \mathbf{M} \cdot (\kappa(\mathbf{v} \times \delta\boldsymbol{\tau}) + \boldsymbol{\tau} \times \delta(\kappa\mathbf{v})). \end{aligned} \tag{79}$$

Further manipulation of the expressions in Eq. (79) yields

$$\begin{aligned}\boldsymbol{\tau} \times \delta(\kappa\mathbf{v}) &= \boldsymbol{\tau} \times (\delta\kappa\mathbf{v} + \kappa\delta\mathbf{v}) = \delta\kappa(\boldsymbol{\tau} \times \mathbf{v}) + \kappa(\boldsymbol{\tau} \times \delta\mathbf{v}) \\ &= \delta\kappa\mathbf{b} + \kappa(\boldsymbol{\tau} \times (-\kappa\boldsymbol{\tau}\delta X)) = \delta\kappa\mathbf{b}, \\ \kappa(\mathbf{v} \times \delta\boldsymbol{\tau}) &= \kappa(\boldsymbol{\tau} \times \delta\mathbf{v}) = \kappa(\boldsymbol{\tau} \times (-\kappa\boldsymbol{\tau}\delta X)) = 0 \end{aligned} \tag{80}$$

and reduces the virtual work to

$$\delta W = -\int_0^L \mathbf{M} \cdot \delta\kappa\mathbf{b}. \tag{81}$$

The variation of the curvature κ, Eq. (81), can be rewritten as

$$\delta(\mathbf{t} \times \mathbf{t}') = \delta(\mathbf{t} \times (\kappa\mathbf{n})) = \delta(\kappa(\mathbf{t} \times \mathbf{n})) = \delta\kappa\mathbf{b} + \kappa\underbrace{\delta\mathbf{b}}_{0} = \delta\kappa\mathbf{b}. \tag{82}$$

Application of the assumptions by Troger and Steindl [10, Eq. (L.11)] gives

$$\mathbf{M} = \mathrm{EI}(\boldsymbol{\tau} \times \boldsymbol{\tau}') \tag{83}$$

and yields the virtual work in the form that directly corresponds to Eq. (18) of the present paper

$$\delta W = -\mathrm{EI} \int_0^L (\boldsymbol{\tau} \times \boldsymbol{\tau}') \cdot \delta(\boldsymbol{\tau} \times \boldsymbol{\tau}') \tag{84}$$

indicating that the model introduced by Troger and Steindl is fully compatible to the potential energy applied in the extended Lagrange equations of the present work.

References

[1] M.P. Païdoussis, *Fluid–structure Interactions, Slender Structures and Axial Flow*, Vol. 1, Academic Press, San Diego, 1998.
[2] C. Semler, G.X. Li, M.P. Païdoussis, The non-linear equations of motion of pipes conveying fluid, *Journal of Sound and Vibration* 169 (5) (1994) 577–599.
[3] M.P. Païdoussis, G.X. Li, Pipes conveying fluid: a model dynamical problem, *Journal of Fluids and Structures* 7 (1993) 137–204.
[4] M. Stangl, N.A. Beliaev, A.K. Belyaev, H. Irschik, Applying Lagrange equations and Hamilton's principle to vibrations of fluid conveying pipes, *Proceedings of XXXIII Summer School APM*, St. Petersburg, Russia, 2005, pp. 269–275.
[5] M. Stangl, H. Irschik, Vibrations of pipes with internal flow and rigid body degrees of freedom, *Proceedings in Applied Mathematics and Mechanics* 5 (2005) 137–138.
[6] M. Stangl, H. Irschik, Dynamics of a Euler elastica pipe with internal flow of fluid, *Proceedings in Applied Mathematics and Mechanics* 6 (2006) 335–336.
[7] M. Nikolic, M. Rajkovic, Bifurcations in nonlinear models of fluid-conveying pipes supported at both ends, *Journal of Fluids and Structures* 22 (2006) 173–195.
[8] C.N. Folley, A.K. Bajaj, Spatial nonlinear dynamics near principal parametric resonance for a fluid-conveying cantilever pipe, *Journal of Fluids and Structures* 21 (2005) 459–484.
[9] C.N. Folley, A.K. Bajaj, *Nonlinear Flow-induced Vibration of Structures, Stability of Gyroscopic Systems*, World Scientific, Singapore, 1999, pp. 1–102.
[10] H. Troger, A. Steindl, *Nonlinear Stability and Bifurcation Theory*, Springer, Wien, 1991.
[11] T.S. Lundgren, P.R. Sethna, A.K. Bajaj, Stability boundaries for flow induced motions of tubes with an inclined nozzle, *Journal of Sound and Vibration* 64 (1979) 553–571.
[12] T.B. Benjamin, Dynamics of a system of articulated pipes conveying fluid, I. Theory, *Proceedings of the Royal Society of London* 261 (1961) 457–486.
[13] H. Irschik, H.J. Holl, The equations of Lagrange written for a non-material volume, *Acta Mechanica* 153 (2002) 231–248.
[14] J. Gerstmayr, M. Stangl, High-order implicit Runge–Kutta methods for discontinuous mechatronical systems, *Proceedings of XXXII Summer School APM*, St. Petersburg, Russia, 2004, pp. 162–169.
[15] K.D. Hjelmstad, *Fundamentals of Structural Mechanics*, second ed., Springer Science, New York, 2005.
[16] S.I. Lee, J. Chung, New non-linear modeling for vibration analysis of a straight pipe conveying fluid, *Journal of Sound and Vibration* 254 (2) (2002) 313–325.
[17] R.H. Plaut, Postbuckling and vibration of end-supported elastica pipes conveying fluid and columns under follower loads, *Journal of Sound and Vibration* 289 (2006) 264–277.
[18] J.C. Simo, L. Vu Quoc, On the dynamics of flexible beams under large overall motions—the plane case: part I, *Journal of Applied Mechanics* 53 (1986) 849–863.
[19] L.E. Malvern, *Introduction to the Mechanics of a Continuous Medium*, Prentice-Hall, Englewood Cliffs, NJ, 1969.
[20] I.H. Stampouloglou, E.E. Theotokoglou, P.N. Andriotaki, Asymptotic solutions to the non-linear cantilever elastica, *International Journal of Non-linear Mechanics* 40 (2005) 1252–1262.
[21] A.A. Shabana, *Dynamics of Multibody Systems*, third ed., Cambridge University Press, Cambridge, 2005.
[22] L.R. Petzold, *A Description of DASSL: A Differential/Algebraic System Solver*, Scientific Computing, Amsterdam, 1983.
[23] E. Hairer, G. Wanner, *Solving Ordinary Differential Equations, Stiff and Differential-Algebraic Problems*, second ed., Springer Series in Computational Mathematics, 1996.
[24] G. Hamel, *Theoretische Mechanik*, Springer, Berlin, 1949.
[25] O.C. Zienkiewicz, R.L. Taylor, *The Finite Element Method. Vol. 1: The Basis*, fifth ed., Butterworth Heinemann, London, 2000.
[26] J. Carr, *Application of the Center Manifold Theory*, Springer, New York, 1981.
[27] J. Guckenheimer, P. Holmes, *Nonlinear Oscillations, Dynamical Systems, and Bifurcation of Vector Fields*, Springer, Berlin, 1990.
[28] J. Gerstmayr, A.A. Shabana, Analysis of thin beams and cables using the absolute nodal coordinate formulation, *Journal of Nonlinear Dynamics* 45 (2006) 109–130.
[29] M. Stangl, J. Gerstmayr, H. Irschik, A large deformation finite element for pipes conveying fluid based on the absolute nodal coordinate formulation, *Proceedings of the ASME 2007 International Design Engineering Technical Conferences & Computers and Information in Engineering Conference IDETC/CIE 2007*, Las Vegas, Nevada, USA, 2007, Paper no. DETC2007-34771, accepted for publication.
[30] S.A.Q. Siddiqui, M.F. Golnaraghi, G.R. Heppler, Dynamics of a flexible cantilever beam carrying a moving mass, *Journal of Nonlinear Dynamics* 15 (1998) 137–154.